Geochemical Perspectives Letters EAG

Barium isotope evidence for a magmatic fluid-dominated petrogenesis of LCT-type pegmatites

G. Deng, D. Jiang, G. Li, Z. Xu, F. Huang

Supplementary Information

The Supplementary Information includes:

- Geological Background and Samples
- Analytical Method
- Simulation of Magmatic Fluid Mixing with Highly Differentiated Melts
- Figures S-1 and S-2
- Tables S-1 to S-3
- Supplementary Information References

Geological Background and Samples

The Sonpan-Ganze orogenic belt (SGOB) is located in the northeastern margin of the Tibetan Plateau and stretches east-west for more than 2800 km (Xu *et al.*, 2020). The SGOB formed during the Middle to Late Triassic closure of the Paleo-Tethys Ocean, and overall exhibits a distinctive triangular shape (Yin and Harrison, 2000). It is bounded by the Kunlun-Qaidam Terrane to the north, the Qiangtang Terrane to the south, and the Yangtze Block to the east (Xu *et al.*, 2020). A large number of 228–195 Ma syn- and post-orogenic granites are widely developed within the SGOB, and the Sr-Nd isotope compositions indicate that the magma should be mainly derived from partial melting of the basement rocks and cover sediments of the orogenic belt in the source, with a small contribution from mantle derived material (Roger *et al.*, 2004; Zhang *et al.*, 2006). Recently, several large to super-large pegmatite Li-Be deposits have been discovered in the eastern part of the SGOB, constituting an important mineralization zone of rare metals (Huang *et al.*, 2020; Zheng *et al.*, 2020). These pegmatite Li-Be deposits are hosted within gneiss domes such as Jiajika, Danba, Markam, Keeryin and Zawulong, which are characterized by Triassic granite cores enveloped by Triassic metamorphic rocks (Xu *et al.*, 2020).

The Jiajika gneiss dome has a core of Majingzi two-mica granite and a set of Triassic metasedimentary rocks in the mantle. The Majingzi two-mica granite belongs to peraluminous S-type granite, with an exposed area of about 5.5 km^2 (Huang *et al.*, 2020). The metasedimentary rocks are the result of high-temperature, meddle-low pressure metamorphism of the Xikang Group strata. They are well-zoned surrounding the Majingzi granite, with sillimanite, staurolite-andalusite, garnet-biotite and sericite-chlorite zones from the interior to the margins (Xu *et al.*, 2020). More than 500 granitic pegmatite veins have been found in the two-mica granite and metasedimentary rocks covering an area of ~60 km^2. These pegmatites can be divided into five zones surrounding the two-mica granite, which are, in order from the pluton outward, microcline pegmatite (I), microcline-albite pegmatite (II), albite pegmatite (III), albite-spodumene pegmatite (IV) and albite-lepidolite pegmatite (V). However, these pegmatite veins generally lack obvious internal zonation (Huang *et al.*, 2020), with only a few showing simple zonation (wall and inner zone) (Zhao *et al.*, 2021). They typically show sharp contact with wall-rocks (Zhang *et al.*, 2021). Previous studies have shown that the Majingzi granite and the pegmatites were mainly emplaced at ~223–208 Ma and ~216.3–215.5 Ma, respectively (Huang *et al.*, 2020). Li mineralization is mainly developed within zones IV and V, as well as some veins in zone III, with a total estimated Li_2O reserves of up to 3.0 Mt, ranking the first in Asia (Huang *et al.*, 2020). Li mineralized pegmatites typically comprise mainly albite, microcline, spodumene, quartz, muscovite, calcite, and chlorite, with minor minerals such as apatite, beryl, zircon, cookeite, cassiterite, and columbite-tantalite (Wang *et al.*, 2023). In addition, Be mineralization can be observed in some pegmatite veins of zones I and II (Huang *et al.*, 2020).

The borehole samples used in this study are from the Jiajika Scientific Drilling (JSD-1) project (Xu *et al.*, 2023). The drill hole was located ~1 km away to the northeast of the Majingzi granite (101°16′39.34″ E, 30°17′16.31″ N), at an altitude of 4425 m, and was drilled to a final depth of 3211.21 m. The JSD-1 core consists of 35 % metasediments, 14 % granite-aplites and 51 % pegmatites. The metasedimentary rocks can be divided into two unites. The upper unit (<900 m in depth) is mainly schists, while the lower unit contains metamorphic calc-silicate rocks and biotite schists. Two granite sheets are identified at the depths of 418–440 m and 1245–1455 m, respectively. The greyish-white two-mica granites typically consist of quartz (35–40 %), microcline (20–30 %), albite (20–30 %), minor muscovite (1–5 %), and biotite (1–5 %) (Luo *et al.*, 2024). Corresponding to the classification of metasedimentary rocks, aplites can also be divided into two categories. Layered aplites mostly occur at depths less than 900 m and consist of dark and light oscillating bands, with plagioclase and quartz in the light layers and additional tourmaline and garnet in the dark layers. Whereas, below 900 m, the aplites generally lack apparent layering (Xu *et al.*, 2023). The mineral composition of pegmatites varies significantly with depth. Spodumene, the only Li-rich mineral, is present only in albite-spodumene pegmatites at depths less than 100 m. This leads to a dramatic increase in the whole-rock Li contents of pegmatites (from ~40 μg/g to 6000 μg/g) (Xu *et al.*, 2023). The spodumene-barren pegmatites are widely distributed below 100 m, with the main mineral compositions of microcline, albite, quartz, muscovite, biotite, tourmaline, beryl, and garnet. A gradual decrease in microcline and biotite with a gradual increase in albite and tourmaline are observed in the pegmatites from bottom to top along JSD-1 core. In addition to Li, the contents of other rare metal elements in the pegmatites also increase markedly from different depths (*e.g.*, Be < 800 m, Nb, Ta < 1700 m) (Jin *et al.*, 2023). Monazite and columbite-group minerals U-Pb dating results showed that most pegmatites in JSD-1 core have a similar age range (213–205 Ma) to the granites (208–205 Ma) (Zhou *et al.*, 2023; Zhu *et al.*, 2023). Some younger albite pegmatites (193–190 Ma) with Nb-Ta mineralization were additionally observed at depths of 3170–3211 m, suggesting at least two episodes of magmatic-hydrothermal events (Jin *et al.*, 2023; Zhou *et al.*, 2023; Zhu *et al.*, 2023).

Analytical Method

In this study, 32 granitic pegmatites, 11 granitic aplites, 4 granites and 19 metasedimentary wall-rocks were collected from different depths of the JSD-1 core. For pegmatites, in order to avoid possible sampling bias due to their coarse crystals, each sample contained as far as possible a representative mineral assemblage of the sampled pegmatites.

Barium isotopes were analysed at the CAS Key Laboratory of Crust-Mantle Materials and Environments in the University of Science and Technology of China. Nan *et al.* (2015, 2018) described in detail the sample dissolution, chemical purification, and instrumental measurement, and the brief description is as follows. Sample powders containing ~2 µg Ba were dissolved with a 3:1 (v/v) mixture of HF–HNO_3 in 7 mL Teflon PFA screw-top beakers (Savillex). After drying, the samples were treated with aqua regia and concentrated HCl to remove fluorides. Barium was purified from the matrix using cation exchange resin (AG50W-X12, 200–400 mesh, Bio-Rad, USA). Ba was collected with 3 mol/L HNO_3 after eluting the matrix elements using 3 mol/L HCl. The purified samples were dried and diluted with 2 % HNO_3 for measurement. The yields of the purification process were >99 % and the total procedural blank was <5 ng. Ba isotope compositions were measured on a Neptune-Plus multi-collector inductively coupled plasma mass spectrometer (MC-ICP-MS, Thermo-Fisher Scientific). Instrumental mass discrimination was corrected using the ^{135}Ba–^{136}Ba double-spike method. Sample solutions were introduced with an Aridus II desolvator (CETAC Technologies, USA) to reduce the formation of polyatomic ions (e.g., BaO^+) and increase sensitivity (~30 V/100 ng/g for ^{138}Ba). Normal Ni sampler and Ni X skimmer cones and the low-resolution mode were adopted for measurement, with ^{134}Ba, ^{135}Ba, ^{136}Ba, ^{137}Ba and ^{138}Ba collected simultaneously by the L2, L1, C, H1 and H2 Faraday cups, respectively. ^{131}Xe and ^{140}Ce were also collected by L4 and H3 Faraday cups, respectively, to correct the effects of isobaric interferences. The background signals for ^{138}Ba (<0.02 V) were negligible relative to the sample signals.

Simulation of Magmatic Fluid Mixing with Highly Differentiated Melts

To further decipher the exact mechanism of magmatic fluid participation in pegmatite formation, a model of magmatic fluid mixing with highly differentiated melt is developed in $\delta^{138/134}$Ba–Ba diagram. The magmatic fluids exsolved from the underlying magma reservoirs, and their Ba contents and Ba isotope compositions can be calculated by respective Rayleigh fractionation equations:

$$C_{\text{fluid}} = C_0 \cdot [1-(1-F)^D]/F \tag{S-1}$$

$$\delta^{138/134}\text{Ba}_{\text{fluid}} = (\delta^{138/134}\text{Ba}_0 + 1000)(f^{\alpha} - 1) / (f-1) - 1000 \tag{S-2}$$

where C_0 and $\delta^{138/134}\text{Ba}_0$ are the Ba content and Ba isotope composition of the initial melt, respectively, represented by the average of granite and aplite samples (except for sample J018509 with obviously lower $\delta^{138/134}$Ba), and F and f are the fractions of fluid exsolution and Ba remaining in the melt, respectively, and D and α are the bulk partition coefficient and the equilibrium fractionation factor between fluid and melt, respectively. The D and α are calculated based on the regression equations involving temperature, fluid salinity, and melt ASI, obtained experimentally by Guo *et al.* (2020). Temperatures of 650 °C and 600 °C are used because of the long-term cold storage of the shallow magmatic system at near-solidus or even lower temperatures (Rubin *et al.*, 2017; Szymanowski *et al.*, 2017). The fluid salinity and melt ASI are obtained from fluid inclusions and the average of granite and aplite samples, respectively (Table S-2). Since the fluid exsolving proportion in silicate melts is typically less than 10 % (Edmonds and Woods, 2018), the calculated results with a proportion of 10 % (i.e. F = 0.1) are used as the composition ranges of the magmatic fluids. The results show that temperature variation (650 °C and 600 °C) has small influences on the Ba content and $\delta^{138/134}$Ba of the magmatic fluids (Table S-2), so the averages of results corresponding to the two temperatures are used in the subsequent mixing simulation.

As the K-feldspar-controlled crystallization would lead to an elevated $\delta^{138/134}$Ba in the residual melts, the average of aplite samples (except for sample J018509 with obviously lower $\delta^{138/134}$Ba) and two pegmatites with elevated $\delta^{138/134}$Ba and different Ba/Rb ratios covering the main Ba/Rb range of Jiajika pegmatites are selected to represent highly differentiated melts (i.e. C_{melt} and $\delta^{138/134}\text{Ba}_{\text{melt}}$). Then the Ba contents and $\delta^{138/134}$Ba of the mixtures can be described by the respective following mass balance equations:

$$C_{\text{mix}} = f_{\text{fluid}} \cdot C_{\text{fluid}} + (1 - f_{\text{fluid}}) \cdot C_{\text{melt}} \tag{S-3}$$

$$\delta^{138/134}\text{Ba}_{\text{mix}} \cdot C_{\text{mix}} = \delta^{138/134}\text{Ba}_{\text{fluid}} \cdot f_{\text{fluid}} \cdot C_{\text{fluid}} + \delta^{138/134}\text{Ba}_{\text{melt}} \cdot (1 - f_{\text{fluid}}) \cdot C_{\text{melt}} \tag{S-4}$$

where f_{fluid} is the fraction of the mixed magmatic fluids. The calculated results are reported in Table S-3 and are shown in Figure 3d.

Supplementary Figures

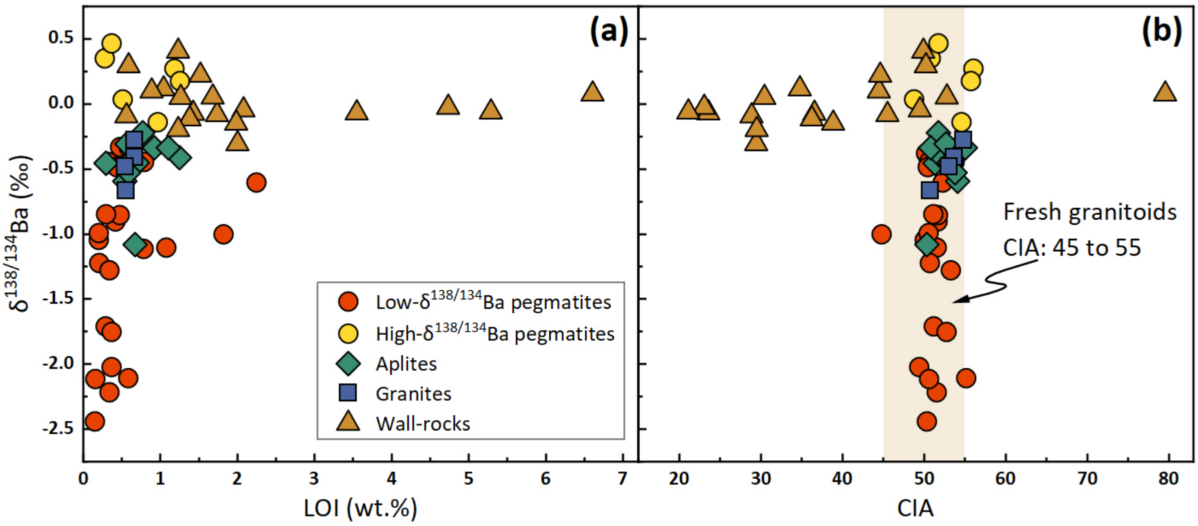

Figure S-1 **(a)** LOI and **(b)** CIA *vs.* $\delta^{138/134}Ba$ for samples from the Jiajika scientific drilling project. Error bar is smaller than the symbols. The CIA range of fresh granitoids comes from Nesbitt and Young (1982).

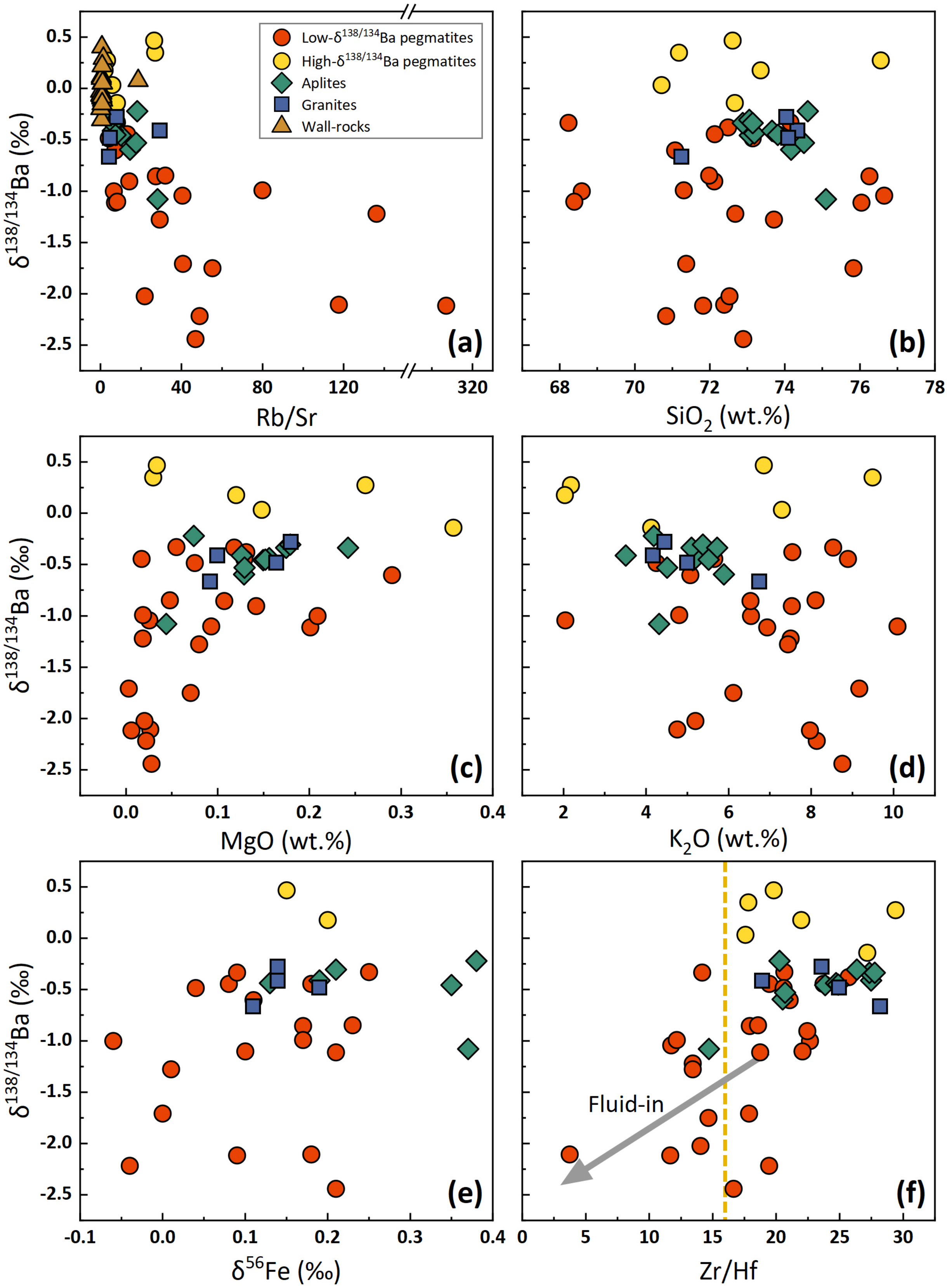

Figure S-2 **(a)** Rb/Sr, **(b)** SiO_2, **(c)** MgO, **(d)** K_2O, **(e)** δ^{56}Fe and **(f)** Zr/Hf *vs.* $\delta^{138/134}$Ba for samples from the Jiajika scientific drilling project. Error bar is smaller than the symbols.

Supplementary Tables

Table S-1 Location and grade data for representative Li deposits worldwide.

Table S-2 Information and Ba isotope compositions of samples from the Jiajika scientific drilling project.

Table S-3 Procedures and results of the quantitative modelling.

Tables S-1 to S-3 are available for download (.xlsx) from the online version of this article at http://doi.org/10.7185/geochemlet.2426.

Supplementary Information References

An, Y.-J., Li, X., Zhang, Z.-F. (2020) Barium Isotopic Compositions in Thirty-Four Geological Reference Materials Analysed by MC-ICP-MS. *Geostandards and Geoanalytical Research* 44, 183–199. https://doi.org/10.1111/ggr.12299

Barnes, E.M., Weis, D., Groat, L.A. (2012) Significant Li isotope fractionation in geochemically evolved rare element-bearing pegmatites from the Little Nahanni Pegmatite Group, NWT, Canada. *Lithos* 132–133, 21–36. https://doi.org/10.1016/j.lithos.2011.11.014

Bowell, R.J., Lagos, L., de los Hoyos, C.R., Declercq, J. (2020) Classification and Characteristics of Natural Lithium Resources. *Elements* 16, 259–264. https://doi.org/10.2138/gselements.16.4.259

Camacho, A., Baadsgaard, H., Davis, D.W., Černý, P. (2012) RADIOGENIC ISOTOPE SYSTEMATICS OF THE TANCO AND SILVERLEAF GRANITIC PEGMATITES, WINNIPEG RIVER PEGMATITE DISTRICT, MANITOBA. *The Canadian Mineralogist* 50, 1775–1792. https://doi.org/10.3749/canmin.50.6.1775

Deng, G., Kang, J., Nan, X., Li, Y., Guo, J., Ding, X., Huang, F. (2021) Barium isotope evidence for crystal-melt separation in granitic magma reservoirs. *Geochimica et Cosmochimica Acta* 292, 115–129. https://doi.org/10.1016/j.gca.2020.09.027

Deng, G., Jiang, D., Zhang, R., Huang, J., Zhang, X., Huang, F. (2022) Barium isotopes reveal the role of deep magmatic fluids in magmatic-hydrothermal evolution and tin enrichment in granites. *Earth and Planetary Science Letters* 594, 117724. https://doi.org/10.1016/j.epsl.2022.117724

Edmonds, M., Woods, A.W. (2018) Exsolved volatiles in magma reservoirs. *Journal of Volcanology and Geothermal Research* 368, 13–30. https://doi.org/10.1016/j.jvolgeores.2018.10.018

Gong, Y., Zeng, Z., Zhou, C., Nan, X., Yu, H., Lu, Y., Li, W., Gou, W., Cheng, W., Huang, F. (2019) Barium isotopic fractionation in latosol developed from strongly weathered basalt. *Science of The Total Environment* 687, 1295–1304. https://doi.org/10.1016/j.scitotenv.2019.05.427

Gou, L.-F., Deng, L. (2019) Determination of Barium Isotopic Ratios in River Water on the Multiple Collector Inductively Coupled Plasma Mass Spectrometer. *Analytical Sciences* 35, 521–527. https://doi.org/10.2116/analsci.18P329

Guo, H., Li, W.-Y., Nan, X., Huang, F. (2020) Experimental evidence for light Ba isotopes favouring aqueous fluids over silicate melts. *Geochemical Perspectives Letters* 16, 6–11. http://dx.doi.org/10.7185/geochemlet.2036

Hu, X.-j., Li, H. (2021) Research progress and prospect of granitic pegmatite-type lithium deposits. *The Chinese Journal of Nonferrous Metals* 31, 3468–3488. https://doi.org/10.11817/j.ysxb.1004.0609.2021-42169

Huang, T., Fu, X., Ge, L., Zou, F., Hao, X., Yang, R., Xiao, R., Fan, J. (2020) The genesis of giant lithium pegmatite veins in Jiajika, Sichuan, China: Insights from geophysical, geochemical as well as structural geology approach. *Ore Geology Reviews* 124, 103557. https://doi.org/10.1016/j.oregeorev.2020.103557

Jin, W., Che, X., Wang, R., Xu, Z., Hu, H., Zhang, R., Li, G., Zheng, B. (2023) The deep rare metal metallogenic characteristics of the Jiajika lithium polymetallic deposit in Sichuan Province, China: Revealed by the Jiajika Scientific Drilling. *Ore Geology Reviews* 160, 105579. https://doi.org/10.1016/j.oregeorev.2023.105579

Kesler, S.E., Gruber, P.W., Medina, P.A., Keoleian, G.A., Everson, M.P., Wallington, T.J. (2012) Global lithium resources: Relative importance of pegmatite, brine and other deposits. *Ore Geology Reviews* 48, 55–69. https://doi.org/10.1016/j.oregeorev.2012.05.006

Kinny, P. (2000) U–Pb dating of rare-metal (Sn–Ta–Li) mineralized pegmatites in Western Australia by SIMS analysis of tin and tantalum-bearing ore minerals. *New Frontiers in Isotope Geoscience Conference,* University of Melbourne, Victoria, February 2000, 113–116.

Krogstad, E.J., Walker, R.J. (1994) High closure temperatures of the U-Pb system in large apatites from the Tin Mountain pegmatite, Black Hills, South Dakota, USA. *Geochimica et Cosmochimica Acta* 58, 3845–3853. https://doi.org/10.1016/0016-7037(94)90367-0

Lasmanis, R. (1978) Lithium resources in the Yellowknife area, Northwest Territories, Canada. *Energy* 3, 399–407. https://doi.org/10.1016/0360-5442(78)90037-3

Liu, L., Wang, D., Liu, X., Li, J., Dai, H., Yan, W. (2017) The main types, distribution features and present situation of exploration and development for domestic and foreign lithium mine. *Geology in China* 44, 263–278. https://doi.org/10.12029/gc20170204

Luo, X.-L., Li, W., Du, D.-H., An, S., Zheng, B., Zhu, W., Xu, Z. (2024) Iron isotope systematics of the Jiajika granite-pegmatite lithium deposit, Sichuan, China. *Ore Geology Reviews* 165, 105903. https://doi.org/10.1016/j.oregeorev.2024.105903

Melcher, F., Graupner, T., Gäbler, H.-E., Sitnikova, M., Henjes-Kunst, F., Oberthür, T., Gerdes, A., Dewaele, S. (2015) Tantalum–(niobium–tin) mineralisation in African pegmatites and rare metal granites: Constraints from Ta–Nb oxide mineralogy, geochemistry and U–Pb geochronology. *Ore Geology Reviews* 64, 667–719. https://doi.org/10.1016/j.oregeorev.2013.09.003

Nan, X., Wu, F., Zhang, Z., Hou, Z., Huang, F., Yu, H. (2015) High-precision barium isotope measurements by MC-ICP-MS. *Journal of Analytical Atomic Spectrometry* 30, 2307–2315. https://doi.org/10.1039/C5JA00166H

Nan, X.-Y., Yu, H.-M., Rudnick, R.L., Gaschnig, R.M., Xu, J., Li, W.-Y., Zhang, Q., Jin, Z.-D., Li, X.-H., Huang, F. (2018) Barium isotopic composition of the upper continental crust. *Geochimica et Cosmochimica Acta* 233, 33–49. https://doi.org/10.1016/j.gca.2018.05.004

Nesbitt, H.W., Young, G.M. (1982) Early Proterozoic climates and plate motions inferred from major element chemistry of lutites. *Nature* 299, 715–717. https://doi.org/10.1038/299715a0

Partington, G.A., McNaughton, N.J., Williams, I.S. (1995) A review of the geology, mineralization, and geochronology of the Greenbushes Pegmatite, Western Australia. *Economic Geology* 90, 616–635. https://doi.org/10.2113/gsecongeo.90.3.616

Roger, F., Malavieille, J., Leloup, Ph.H., Calassou, S., Xu, Z. (2004) Timing of granite emplacement and cooling in the Songpan–Garzê Fold Belt (eastern Tibetan Plateau) with tectonic implications. *Journal of Asian Earth Sciences* 22, 465–481. https://doi.org/10.1016/S1367-9120(03)00089-0

Rubin, A.E., Cooper, K.M., Till, C.B., Kent, A.J.R., Costa, F., Bose, M., Gravley, D., Deering, C., Cole, J. (2017) Rapid cooling and cold storage in a silicic magma reservoir recorded in individual crystals. *Science* 356, 1154–1156. https://doi.org/10.1126/science.aam8720

Simmons, W.B., Falster, A.U., Freeman, G. (2020) The Plumbago North pegmatite, Maine, USA: a new potential lithium resource. *Mineralium Deposita* 55, 1505–1510. https://doi.org/10.1007/s00126-020-00956-y

Szymanowski, D., Wotzlaw, J.-F., Ellis, B.S., Bachmann, O., Guillong, M., von Quadt, A. (2017) Protracted near-solidus storage and pre-eruptive rejuvenation of large magma reservoirs. *Nature Geoscience* 10, 777–782. https://doi.org/10.1038/ngeo3020

van Zuilen, K., Müller, T., Nägler, T.F., Dietzel, M., Küsters, T. (2016) Experimental determination of barium isotope fractionation during diffusion and adsorption processes at low temperatures. *Geochimica et Cosmochimica Acta* 186, 226–241. http://dx.doi.org/10.1016/j.gca.2016.04.049

Wang, G.-G., Zheng, F.-B., Ni, P., Wu, Y.-W., Qi, W.-X., Li, Z.-A. (2023) Fluid properties and ore-forming process of the giant Jiajika pegmatite Li deposit, western China. *Ore Geology Reviews* 160, 105613. https://doi.org/10.1016/j.oregeorev.2023.105613

Xu, Z., Fu, X., Wang, R., Li, G., Zheng, Y., Zhao, Z., Lian, D. (2020) Generation of lithium-bearing pegmatite deposits within the Songpan-Ganze orogenic belt, East Tibet. *Lithos* 354–355, 105281. https://doi.org/10.1016/j.lithos.2019.105281

Xu, Z., Zheng, B., Zhu, W., Chen, Y., Li, G., Gao, J., Che, X., Zhang, R., Wei, H., Li, W., Wang, G., Wei, G., Yan, H. (2023) Geologic Scenario from Granitic sheet to Li-rich Pegmatite Uncovered by Scientific Drilling at the Jiajika Lithium Deposit in Eastern Tibetan Plateau. *Ore Geology Reviews* 161, 105636. https://doi.org/10.1016/j.oregeorev.2023.105636

Yin, A., Harrison, T.M. (2000) Geologic Evolution of the Himalayan-Tibetan Orogen. *Annual Review of Earth and Planetary Sciences* 28, 211–280. https://doi.org/10.1146/annurev.earth.28.1.211

Zhang, H.-F., Zhang, L., Harris, N., Jin, L.-L., Yuan, H. (2006) U–Pb zircon ages, geochemical and isotopic compositions of granitoids in Songpan-Garze fold belt, eastern Tibetan Plateau: constraints on petrogenesis and tectonic evolution of the basement. *Contributions to Mineralogy and Petrology* 152, 75–88. https://doi.org/10.1007/s00410-006-0095-2

Zhang, H., Tian, S., Wang, D., Li, X., Liu, T., Zhang, Y., Fu, X., Hao, X., Hou, K., Zhao, Y., Qin, Y. (2021) Lithium isotope behavior during magmatic differentiation and fluid exsolution in the Jiajika granite–pegmatite deposit, Sichuan, China. *Ore Geology Reviews* 134, 104–139. https://doi.org/10.1016/j.oregeorev.2021.104139

Zhao, H., Chen, B., Huang, C., Bao, C., Yang, Q., Cao, R. (2021) Geochemical and Sr–Nd–Li isotopic constraints on the genesis of the Jiajika Li-rich pegmatites, eastern Tibetan Plateau: implications for Li mineralization. *Contributions to Mineralogy and Petrology* 177, 4. https://doi.org/10.1007/s00410-021-01869-3

Zheng, Y., Xu, Z., Li, G., Lian, D., Zhao, Z., Ma, Z., Gao, W. (2020) Genesis of the Markam gneiss dome within the Songpan-Ganzi orogenic belt, eastern Tibetan Plateau. *Lithos* 362–363, 105475. https://doi.org/10.1016/j.lithos.2020.105475

Zhou, M., Zhang, R., Hanchar, J.M., Xu, Z., Lu, J., Hu, H., Che, X., Zheng, B., Li, G. (2023) Unravelling the genetic relationship between pegmatites and granites in the Jiajika Li-Be polymetallic district, Songpan-Ganze Orogenic Belt, Southwestern China: Insights from monazite U-Pb geochronology and trace element geochemistry. *Ore Geology Reviews* 163, 105774. https://doi.org/10.1016/j.oregeorev.2023.105774

Zhu, J., Zhu, W., Xu, Z., Zhang, R., Che, X., Zheng, B. (2023) The geochronology of pegmatites in the Jiajika lithium deposit, western Sichuan, China: Implications for multi-stage magmatic-hydrothermal events in the Songpan-Ganze rare metal metallogenic belt. *Ore Geology Reviews* 159, 105582. https://doi.org/10.1016/j.oregeorev.2023.105582